

Polymer hot-carrier transistor with low bandgap emitter

Yu-Chiang Chao, Ming-Hong Xie, Ming-Zhi Dai, Hsin-Fei Meng, Sheng-Fu Horng, and Chain-Shu Hsu

Citation: *Applied Physics Letters* **92**, 093310 (2008); doi: 10.1063/1.2839395

View online: <http://dx.doi.org/10.1063/1.2839395>

View Table of Contents: <http://scitation.aip.org/content/aip/journal/apl/92/9?ver=pdfcov>

Published by the [AIP Publishing](#)

Articles you may be interested in

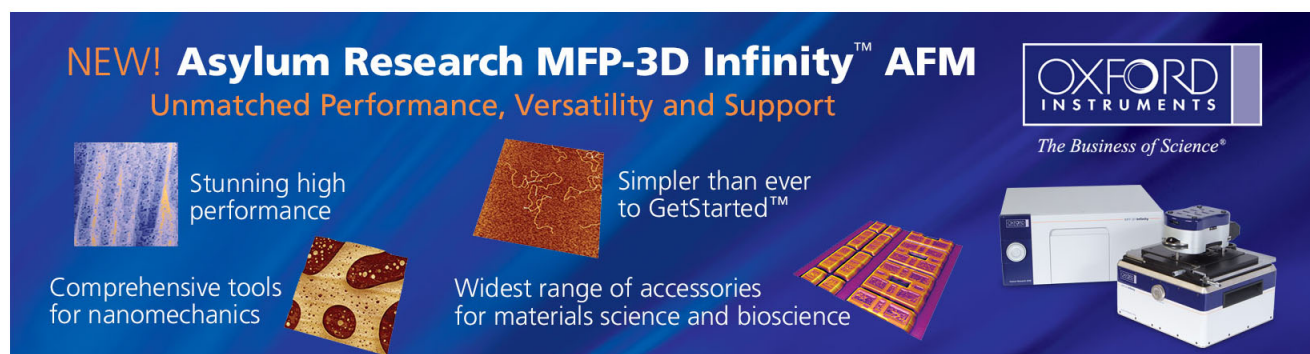
[Flexible low voltage nonvolatile memory transistors with pentacene channel and ferroelectric polymer](#)
Appl. Phys. Lett. **94**, 093304 (2009); 10.1063/1.3089379

[Direct measurement of carrier drift velocity and mobility in a polymer field-effect transistor](#)
Appl. Phys. Lett. **89**, 242104 (2006); 10.1063/1.2405378

[High-density electrostatic carrier doping in organic single-crystal transistors with polymer gel electrolyte](#)
Appl. Phys. Lett. **88**, 112102 (2006); 10.1063/1.2186513

[Short-channel polymer field-effect-transistor fabrication using spin-coating-induced edge template and ink-jet printing](#)
Appl. Phys. Lett. **87**, 232111 (2005); 10.1063/1.2140586

[Close look at charge carrier injection in polymer field-effect transistors](#)
J. Appl. Phys. **94**, 6129 (2003); 10.1063/1.1613369

The advertisement features a dark blue background with a subtle grid pattern. At the top left, the text 'NEW! Asylum Research MFP-3D Infinity™ AFM' is written in white and orange. Below this, the phrase 'Unmatched Performance, Versatility and Support' is written in orange. On the right side, the Oxford Instruments logo is displayed, consisting of the word 'OXFORD' in a large, white, serif font above the word 'INSTRUMENTS' in a smaller, white, sans-serif font, all enclosed in a white rectangular border. Below the logo, the tagline 'The Business of Science®' is written in a smaller, white, sans-serif font. The central part of the advertisement is divided into four quadrants, each containing a small image and a text block. The top-left quadrant shows a blue, textured surface with the text 'Stunning high performance'. The top-right quadrant shows a brown, textured surface with the text 'Simpler than ever to GetStarted™'. The bottom-left quadrant shows a yellow and brown patterned surface with the text 'Comprehensive tools for nanomechanics'. The bottom-right quadrant shows a white and blue AFM instrument with the text 'Widest range of accessories for materials science and bioscience'. The overall design is clean and professional, emphasizing the advanced capabilities and user-friendly nature of the AFM.

Polymer hot-carrier transistor with low bandgap emitter

Yu-Chiang Chao, Ming-Hong Xie, Ming-Zhi Dai, and Hsin-Fei Meng^{a)}
Institute of Physics, National Chiao Tung University, Hsinchu 300, Taiwan

Sheng-Fu Horng

Department of Electrical Engineering, National Tsing Hua University, Hsinchu 300, Taiwan

Chain-Shu Hsu

The Department of Applied Chemistry, National Chiao Tung University, Hsinchu 300, Taiwan

(Received 28 September 2007; accepted 11 January 2008; published online 7 March 2008)

Vertical polymer hot-carrier transistor using the low bandgap material poly(3-hexylthiophene) as both the emitter and the collector are studied. The common emitter current gain is shown to depend on the LiF thickness and the emitter thickness, with maximal value at 31. Current density as high as 31 mA/cm² is achieved when collector voltage is -10 V. For the device using blend of poly(3-hexylthiophene) and high bandgap polymer poly(9-vinylcarbazole) as the emitter, the current density rises sharply to 428 mA/cm². The brightness of 3000 cd/m² is obtained as a polymer light-emitting diode is driven by the transistor with the same area. The transistor can be operated at 100 kHz. © 2008 American Institute of Physics. [DOI: 10.1063/1.2839395]

Conjugated polymers have received great attention because of its applications in light-emitting diode, solar cell, and transistor by solution process. There are two types of polymer transistors, namely, the conventional field-effect transistor (FET) and the vertical metal-based transistor.¹⁻⁶ Due to its potential to overcome the limit of FET, recently metal-base organic transistors, including the space-charge-limited transistor⁴ and hot-carrier transistor,⁵ gain more and more attention for both polymer and small molecules.^{2,3,6,7} Previously, a high bandgap organic semiconductor poly(9-vinylcarbazole) (PVK) is selected for the emitter in order to maximize the energy barrier at the emitter-base junction, thus enhancing the hot-carrier kinetic energy and reducing the base current.⁵ Even though reasonable common emitter current gain β is achieved, the high bandgap emitter comes at a great cost. The high bandgap implies a large barrier for the holes to be injected from the metal contact to the emitter valence band.⁸ Depending on the surface contamination level, the work function of emitter electrode Au can vary from 4.7 to 5.1 eV. The ionization potential of PVK is 5.8 eV, implying a large hole injection barrier of 0.7–1.1 eV. The resulting collector density is therefore as low as 0.56 mA/cm². Similar low current density also occurs in hot-carrier transistor based on evaporated small molecules.⁷

In this work, we replace the high bandgap emitter by a low bandgap polymer poly(3-hexylthiophene) (P3HT) with ionization potential (IP) at 5.1 eV, which is much closer to the Au work function than PVK. In fact, P3HT is also the material used for the collector. There is, therefore, no energy offset between emitter and collector valence band which is usually required for the hot-carrier collection. Similar to the case of PVK emitter, a thin layer of LiF is used as the tunneling barrier to enhance the relative energy. Unlike the PVK device where LiF is only auxiliary to create the hot-carrier energy offset above the collector band edge, for P3HT emitter, the energy offset depends entirely on the LiF layer. The

prerequisite of hot-carrier transistor using low bandgap emitter is, therefore, that the tunneling barrier alone must be able to maintain a good common emitter current gain. It turns out that the common emitter current gain is not compromised even without the high bandgap emitter, indicating that the tunneling barrier is more crucial than the semiconductor band positions for the operation of the transistor. As for the collector current density, it increases dramatically from 0.56 mA/cm² for PVK emitter to several tens of mA/cm² for P3HT emitter. We demonstrate that this transistor is able to drive a polymer light-emitting diode with the same area up to brightness of thousands of cd/m².

The device structure of the hot-carrier transistor in this work is indium tin oxide (ITO)/PEDOT:PSS/P3HT(C)/Al(B)/Al₂O₃/LiF/P3HT(E)/Au. P3HT is used as both the emitter (E) and collector (C). The middle Al layer is the base (B), and the top Au layer is the emitter contact. Figure 1 shows the energy band profile of hot-carrier transistor in the active mode. The thin LiF/Al₂O₃ layer is the tunneling barrier which further separates the emitter valence band and the base Fermi level by a voltage drop across it. The device is fabricated on cleaned ITO substrate, and a 300 Å PEDOT:

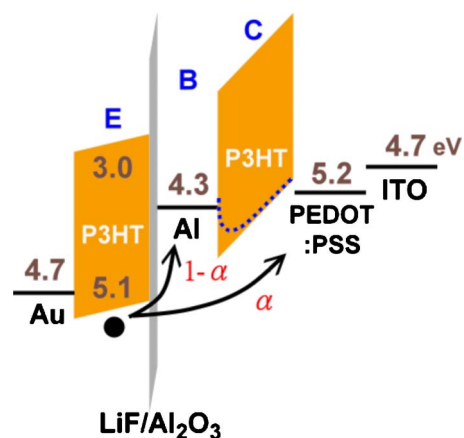


FIG. 1. (Color online) The energy band profile of the polymer hot-carrier transistor in the active mode. The energies are indicated in eV.

^{a)} Author to whom correspondence should be addressed. Electronic mail: meng@mail.nctu.edu.tw.

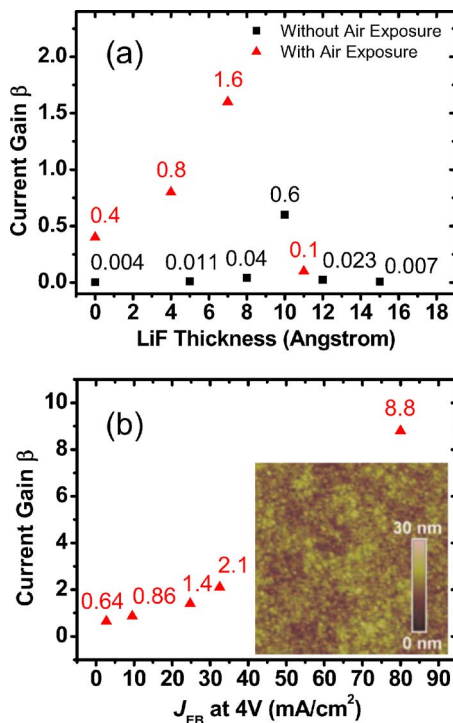


FIG. 2. (Color online) (a) The current gain β as a function of LiF thickness of the hot-carrier transistor. The solid square (solid triangular) indicates the device without (with) exposure to air after Al deposition. The current gain is obtained in the common emitter configuration with V_E is 0 V, V_C is -5 V, and J_B is 2 mA/cm². (b) The current gain β as a function of EB diode current density at 4 V. The current gain is obtained in the common emitter configuration with V_E is 0 V, V_C is -5 V, and J_B is 2.5 mA/cm². The inset shows the AFM image of Al base on P3HT with roughness of 2.6 nm. The height scale is 30 nm and the dimensions of the image is 5 × 5 μm².

:PSS layer is spin coated. P3HT is then spin coated to form the 1200 Å collector layer. A thin Al film around 80 Å is evaporated (10 Å/s) as the base through a shadow mask, followed by a LiF layer of various thicknesses. The optimal Al₂O₃ layer is formed by air exposure for 3 min after Al deposition. The oxidation time for the Al is limited to be 3 min since a 15 Å Al can be completely oxidized in 5 min.⁹ Another P3HT layer is spin coated from xylene (2 wt %) to form 320 Å emitter layer. Au is evaporated as the emitter contact. The active area is 2 mm². The devices are encapsulated by glass cap with UV glue in a glovebox, and measured in ambient condition. The sign convention throughout the text is that when holes leave from the base and collector, J_B and J_C are positive.

Figure 2(a) shows the β of hot-carrier transistor with different LiF layer thicknesses with or without Al₂O₃ layer in the common emitter configuration. For transistor without Al₂O₃, β initially increases with increasing LiF thickness, and reaches a maximum $\beta=0.6$ when LiF thickness is 10 Å. For LiF thickness higher than 10 Å, β decreases due to the insulating nature of LiF. For the transistor with Al₂O₃, β also has a maximum value of 1.6 when LiF thickness is 7 Å. The inset in Fig. 2(b) shows the atomic force microscopy (AFM) image of Al base on P3HT. No pinhole can be observed. In addition, the roughness of 2.6 nm is much smaller than the mean thickness of the Al base.

As LiF thickness increases, the tunneling barrier forms gradually, and the voltage drop across the LiF layer develops. Hence, the energy barrier at emitter-base junction is enlarged and the hot-carrier loss to base reduced. However,

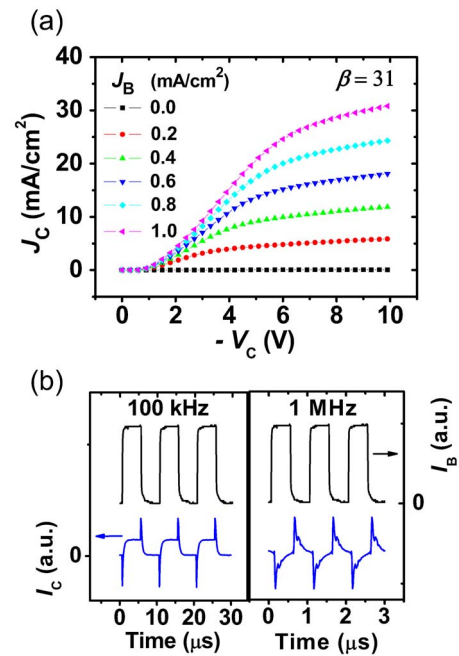


FIG. 3. (Color online) (a) The characteristics of the polymer hot-carrier transistor in common emitter configuration. The emitter layer is P3HT. (b) Frequency response of the hot-carrier transistor under modulation at 100 kHz and 1 MHz.

as the thickness is too large, the LiF layer becomes an insulator which blocks all carriers and the collector current density J_C becomes very small. The residual base current due to the reverse current of the base-collector diode then dominates and causes a small β . In general, β is much higher for devices with Al₂O₃ layer, and the maximal β occurs at smaller LiF thickness. The transistor with Al₂O₃ needs less LiF to achieve maximal β since there is a ultrathin Al₂O₃ before LiF deposition. The Al₂O₃ grown in air is dense with a much better insulating property than LiF, so it may serve as a better tunneling barrier than LiF. Furthermore, the Al₂O₃ may prevent the reaction between Al and LiF which will release Li atom and reduce the thickness of the LiF.¹⁰

In addition to insulator thickness, β is also sensitive to the emitter thickness. A series of hot-carrier transistor with Al₂O₃ and 7 Å LiF, with various emitter thicknesses from 600 to 250 Å is fabricated. The emitter-base diode is fixed at a forward bias $V_{EB}=V_E-V_B$ of 4 V. The emitter-base diode current density J_{EB} increases from 2.7 to 80 mA/cm² as the emitter thickness decreases from 600 to 250 Å. Figure 2(b) shows the relationship between β and J_{EB} . The β increases with increasing J_{EB} and decreasing emitter thickness. The highest $\beta=8.8$ is obtained when J_{EB} is around 80 mA/cm² at 4 V. Initially, V_{EB} increases with increasing $|V_C|$ then saturates. V_{EB} at $V_C=-10$ V and $J_B=2.5$ mA/cm² decreases from 3.9 to 2.5 V with decreasing emitter thickness. For thin thickness, a small V_{EB} is needed to obtain a specific J_B , so base-collector voltage $V_{BC}=V_B-V_C$ is larger for given V_C . The image-force lowering effect at the base collector becomes strong, as shown by the dotted line in Fig. 1. The effective barrier between the base and collector is therefore reduced further and hot-carrier collection more efficient.

Under optimal conditions, the characteristics of the hot-carrier transistor using P3HT as both the emitter and collector is shown in Fig. 3(a). With the lower injection barrier from the Au anode, the collector current density J_C reaches

as high as 31 mA/cm^2 , a dramatic increase from the previous work using high bandgap emitter PVK by two orders of magnitude.⁵ β is 31. This value is similar to the case of PVK suggesting that the hot-carrier collection is not compromised by the lower hot-carrier energy as long as LiF layer is used. Even though there is no energy offset between the emitter and the collector semiconductor, Fig. 3(a) shows that the tunneling barrier alone is enough to produce a reasonable β with proper thickness. The transistor shows quite pronounced saturation as the collector voltage increases. In addition to high β and density, hot-carrier transistor has an intrinsic fast response because the effective channel length is defined by the film thickness which is only 150 nm. Figure 3(b) shows the response of the transistor under modulation at 100 kHz and 1 MHz square wave applied between the base and emitter. The collector current is registered by the voltage across a 100Ω resistor in series. The collector current follows the square wave up to 100 kHz. At 1 MHz, the output waveform is distorted but still responding. Polymer hot-carrier transistor is, therefore, promising for high speed applications in the radio frequency.

Finally, we study the hot-carrier transistor whose emitter is a blend of low and high bandgap materials. P3HT and PVK are blended in toluene solution (1:5 wt/wt) with the total polymer concentration of 6 wt% and spin coated at 8000 rpm to form the emitter. The current density of emitter-base diode at $V_{EB}=4 \text{ V}$ is 126 mA/cm^2 . This transistor is measured in the common emitter configuration when $V_E=0 \text{ V}$, $V_C=-10 \text{ V}$, and $J_B=5 \text{ mA/cm}^2$. The collector current density J_C is 126 mA/cm^2 , β is 25, and on/off ratio is 468. When J_B increases to 40 mA/cm^2 , the output current density is as high as 428 mA/cm^2 , β is 11, and on/off ratio is 1751. Unlike pure P3HT transistor in Fig. 3(a), the blend transistor in Fig. 4(a) somehow does not show a tendency for saturation. AFM image shows a rough surface with root-mean-square value of 20 nm. The roughness may increase the contact area between Au and emitter. In addition, some carriers could be injected stepwise from Au to P3HT, and then finally to PVK. The hot carriers in metal base from PVK have higher energy than those from P3HT, and are easier to cross the base-collector junction barrier and contribute to the collector current.

Now, the current density of the hot-carrier transistor is high enough to drive a PLED, the ITO collector of the hot-carrier transistor and the ITO anode of the PLED are connected to demonstrate their integration. The PLED has the structure ITO/PEDOT/PPV(SuperYellow)/CsF/Al. The Au electrode of hot-carrier transistor is grounded, and the cathode voltage of the PLED is kept constant at -10 V . Figure 4(b) shows the luminance of the PLED at various J_B . The luminance of the PLED driven by the hot-carrier transistor can be over 3000 cd/m^2 , which is enough for most applications.

In conclusion, we show that the high bandgap semiconductor is not necessary for the emitter in organic hot-carrier

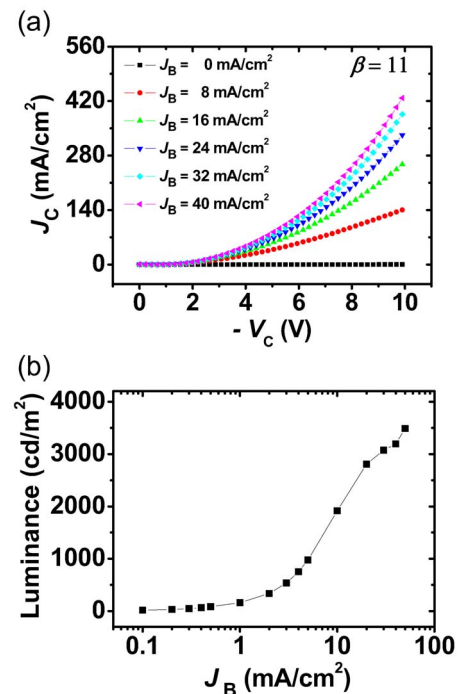


FIG. 4. (Color online) (a) The characteristics of the polymer hot-carrier transistor in common emitter configuration. The emitter layer composed of P3HT and PVK in weight ratio 1:5. (b) The luminance of the polymer light-emitting diode driven by the polymer hot-carrier transistor operated in various base current densities.

transistor in order to achieve a high common emitter current gain. Now, the hot-carrier transistor is good enough to drive a polymer light-emitting diode to high brightness, and it can be operated at a high frequency.

This work was supported by the National Science Council of the Republic of China under Contract No. NSC96-2112-M-009-036.

¹Y. Yang and A. J. Heeger, *Nature (London)* **372**, 344 (1994).

²S. Fujimoto, K. Nakayama, and M. Yokoyama, *Appl. Phys. Lett.* **87**, 133503 (2005).

³K. Fujimoto, T. Hiroi, K. Kudo, and M. Nakamura, *Adv. Mater. (Weinheim, Ger.)* **19**, 525 (2007).

⁴Y. C. Chao, H. F. Meng, and S. F. Horng, *Appl. Phys. Lett.* **88**, 223510 (2006).

⁵Y. C. Chao, S. L. Yang, H. F. Meng, and S. F. Horng, *Appl. Phys. Lett.* **87**, 253508 (2005).

⁶M. Yi, S. Yu, C. Feng, T. Zhang, D. Ma, M. S. Meruvia, and I. A. Hümmelgen, *Org. Electron.* **8**, 311 (2007).

⁷S. S. Cheng, C. Y. Yang, Y. C. Chuang, C. W. Ou, M. C. Wu, S. Y. Lin, and Y. J. Chan, *Appl. Phys. Lett.* **90**, 153509 (2007).

⁸S. C. Tse, S. W. Tsang, and S. K. So, *J. Appl. Phys.* **100**, 063708 (2006).

⁹F. Li, H. Tang, J. Anderegg, and J. Shinar, *Appl. Phys. Lett.* **70**, 1233 (1997).

¹⁰S. E. Shaheen, G. E. Jabbour, M. M. Morrell, Y. Kawabe, B. Kippelen, N. Peyghambarian, M. F. Nabor, R. Schlaf, E. A. Mash, and N. R. Armstrong, *J. Appl. Phys.* **84**, 2324 (1998).